Journal of Inorganic Biochemistry 118 (2013) 74–82

Contents lists available at SciVerse ScienceDirect

Journal of Inorganic Biochemistry

journal homepage: www.elsevier.com/locate/jinorgbio

Ruthenium arene complexes as HIV-1 integrase strand transfer inhibitors

Mauro Carcelli [a,*], Alessia Bacchi [a], Paolo Pelagatti [a], Gabriele Rispoli [a], Dominga Rogolino [a], Tino W. Sanchez [c], Mario Sechi [b], Nouri Neamati [c]

[a] Dipartimento di Chimica, Università di Parma, Parco Area delle Scienze 17/A, 43124 Parma, Italy
[b] Dipartimento di Chimica e Farmacia, Università di Sassari, Via Vienna 2, 07100 Sassari, Italy
[c] Department of Pharmacology and Pharmaceutical Sciences, University of Southern California, School of Pharmacy, 1985 Zonal Avenue, Los Angeles, CA 90089, USA

ARTICLE INFO

Article history:
Received 23 July 2012
Received in revised form 19 September 2012
Accepted 21 September 2012
Available online 28 September 2012

Keywords:
HIV integrase
Strand transfer inhibitor
Metal complex
Ru complex

ABSTRACT

The quinolone HL^1 and the hydroxypyrimidine-carboxamide HL^2 were designed and synthesized as models of the HIV integrase strand transfer inhibitors Elvitegravir and Raltegravir (brand name Isentress), with the aim to study their complexing behavior and their biological activity. The Ru(arene) complexes [RuCl(η^6-*p*-cym)L^1], [RuCl(η^6-*p*-cym)L^2] and [RuCl(hexamethylbenzene)L^2] were also synthesized and spectroscopically characterized and their X-ray diffraction structures were discussed. The ligands and the complexes showed inhibition potency in the sub/low-micromolar concentration range in anti-HIV-1 integrase enzymatic assays, with selectivity toward strand transfer catalytic process, without any significant cytotoxicity on cancer cells.

1. Introduction

The pharmacological properties of metal-based compounds are a topic of great interest in drug discovery, since they have found very important clinical applications [1,2]. The cytoxicity of metal complexes has been extensively investigated [2,3], but the research on their antiviral properties remains scarce [4]. In particular, ruthenium(II) arene complexes have received much attention in the last years, because they are promising candidates in cancer treatment [2,5,6], also thanks to their low toxicity and the peculiar activity against platinum-resistant tumors. On the contrary, in the literature very few studies are available about the antiviral activity of ruthenium compounds and, in particular, about their activity toward HIV-1 infection/replication [4,7–9]. Therefore, in line with our recent research [10–13], we have decided to evaluate the activity of some ruthenium(II) η^6-arene compounds in the inhibition of the enzyme HIV-1 Integrase (IN).

IN, which catalyzes the integration of proviral cDNA into the host cell genome [14–16], has emerged as a promising target in antiretroviral drug design, and it has been recently validated for the treatment of HIV/AIDS. At least five IN inhibitors have been tested in HIV-infected patients [17,18] and several others are currently under advanced preclinical and long-term toxicity studies. Raltegravir (Chart 1) was the first IN inhibitor to be approved by the US FDA, in late 2007 (brand name Isentress) [19]. The integration process promoted by IN consists of two distinct reactions, 3′-processing (3′-P) and strand transfer (ST). In the first step the enzyme removes a terminal dinucleotide from the viral DNA, generating two CA-3′-hydroxyl recessed ends, which are the reactive intermediates required for the next step. The enzyme, still bound to the 3′-processed viral DNA, translocates to the nucleus of the infected cell as a part of the pre-integration complex. Here ST step occurs, which consists of a trans-esterification reaction of the viral DNA 3′-OH on the phosphodiester backbone of host DNA. In the active site of IN there are two Mg^{2+} ions, which are fundamental for the activity of the enzyme: they are the target of the selective ST inhibitors such as Raltegravir.

Starting from the β-diketoacid family of selective IN ST inhibitors (for example L-731,988, Chart 1), the replacement of the keto-enolic moiety and/or of the carboxylic group with bioisoster groups led to several other classes of potent inhibitors, that retained selectivity for the ST process. Among the others, there are (Chart 1) the keto-enol triazoles (for example S-1360) [14], the naphthyridines (L-870,810) [20,21], the hydroxypyrimidine-carboxamides (MK-0518 or Raltegravir) [22,23], the quinolone-carboxylic acids (GS-9137 or Elvitegravir) [24,25], and the pyrido-pyrazino oxazine derivatives (S/GSK1349572) [26]. All these selective IN ST inhibitors share a common scaffold that is able to chelate metal ions, in accordance with the "two-metal binding model" [27] that emerged as an important strategy for the development of IN inhibitors [28].

Quinolones are well-known antibacterial agents, since they are able to inhibit the bacterial DNA gyrase [29,30]. Their biological

* Corresponding author at: Dipartimento di Chimica, Università di Parma Campus Universitario — V.le G.P.Usberti 17/A, 43124 Parma, Italy. Tel.: +39 0521 905427; fax: +39 0521 905557.
E-mail address: mauro.carcelli@unipr.it (M. Carcelli).

0162-0134/$ – see front matter © 2012 Elsevier Inc. All rights reserved.
http://dx.doi.org/10.1016/j.jinorgbio.2012.09.021

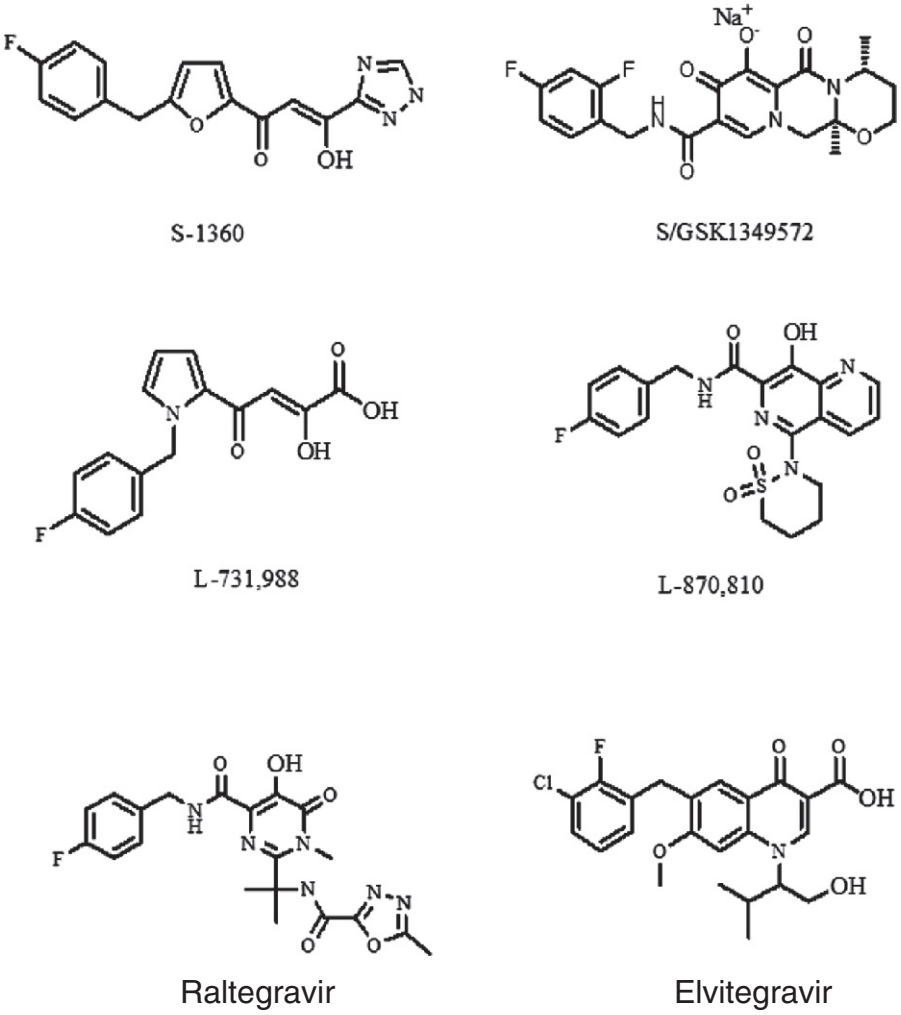

Chart 1. Representative HIV-1 IN ST inhibitors.

activities were extensively explored [31–33] and also their interactions with metals [34–38], and in particular with Mg^{2+}, that is probably involved in the mechanism of action [39]. However, few examples of ruthenium complexes with this class of ligands are known [40–43] and none of them has been tested for antiviral activity. As far as the coordinating behavior of the hydroxypyrimidinecarboxamide moiety of Raltegravir is concerned, also in this case few literature data can be found [13,44]. Moreover, the strategy to use biologically active ligands with ruthenium arene moiety has been already successfully exploited [45,46].

With these considerations in mind, we synthesized some new ruthenium(II) arene compounds with ligands chosen as a model of the quinolone Elvitegravir (HL^1, 6-benzyl-1-(2-hydroxyethyl)-4-oxo-1,4-dihydroquinoline-3-carboxylic acid) and as a model of Raltegravir (HL^2, *N*-(4-fluorobenzyl)-5-hydroxy-1-methyl-2-(1-methyl-1-{[(5-methyl-1,3,4-oxadiazol-2-yl)carbonyl]amino}ethyl)-6-oxo-1,6-dihydropyrimidine-4-carboxamide) (Scheme 1). The model ligands are relatively easy to prepare and yet they retain the pharmacophoric motif of the parent HIV IN inhibitors [13].

Herein we report on the synthesis and the characterization of the organometallic compounds [RuCl(η^6-*p*-cymene)L^1] **(3)**, [RuCl(η^6-*p*-cymene)L^2] **(4)** and [RuCl(η^6-hexamethylbenzene)L^1] **(5)** (Scheme 2), with the discussion of the crystal structure of **(3)** and **(4)**. Finally, the anti-HIV-1 IN enzymatic activity of the free ligands and of the corresponding ruthenium *p*-cymene complexes as well as their cytotoxic effect toward a model cancer cell line, were evaluated.

2. Experimental

2.1. Material and methods

Solvents and reagents were purchased from Sigma-Aldrich, Merck or Carlo Erba and used without further purification. All reactions were performed under a nitrogen atmosphere by using standard Schlenk technique and syringes to transfer solutions. Purity of compounds was determined by elemental analysis and verified to be ≥95% for all synthesized molecules. Elemental analyses were performed by using a Carlo Erba Model EA 1108 apparatus. Nuclear Magnetic Resonance (NMR) spectra were recorded at 27 °C on a Bruker Avance 400 FT spectrophotometer by using $SiMe_4$ as internal standard; the assignment of exchangeable protons (O*H* and N*H*) was confirmed by the addition of D_2O. IR spectra were obtained with a Nicolet 5PCFT-IR spectrophotometer in the 4000–400 cm^{-1} range, in reflectance mode on the powder. Mass spectra were obtained on an attenuated total electrospray ionization (ESI) time-of-flight Micromass 4LCZ spectrometer (ESI/MS).

6-Benzyl-4-oxo-1,4-dihydroquinolin-3-carboxylate ethyl ester **(1)** (Scheme 3) and HL^2 were synthesized as previously reported [13].

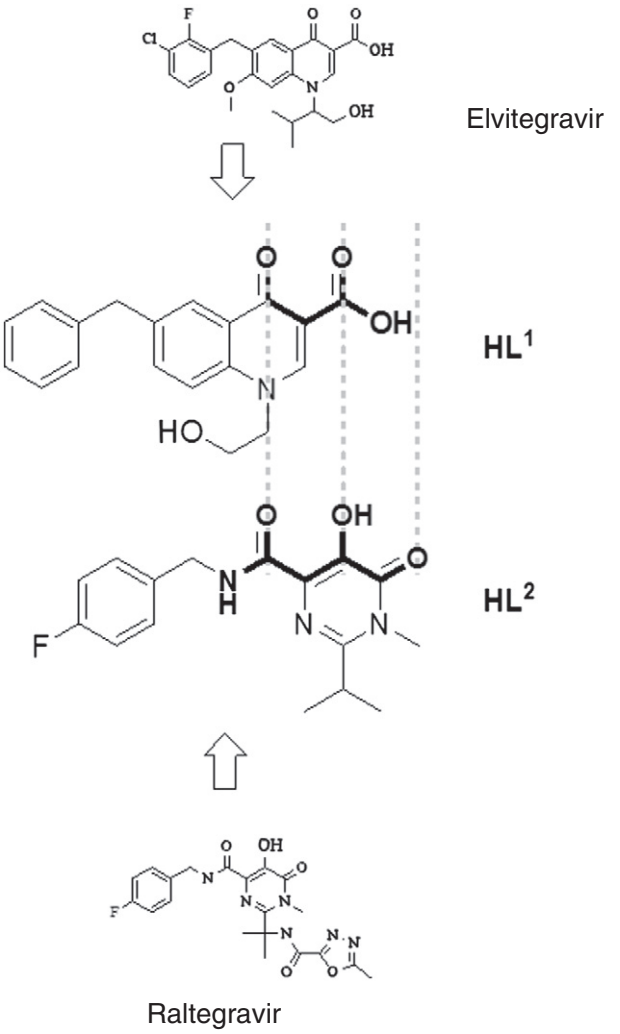

Scheme 1. Chemical structures of the model ligands HL^1 and HL^2.

2.2. Synthesis

6-Benzyl-1-(2-hydroxyethyl)-4-oxo-1,4-dihydroquinoline-3-carboxylate ethyl ester, **(2)**

To a solution of **(1)** (0.61 g, 1.98 mmol) in anhydrous *N,N*-dimethylformamide (13 mL), 60% sodium hydride in oil dispersion (1.5 eq, 0.071 g, 2.98 mmol) and iodoethanol (1.5 eq, 0.510 g, 2.97 mmol, 0.231 mL) were added at room temperature. The resulting mixture was stirred at 90 °C for 24 h. The reaction was cooled and quenched with water. The mixture was acidified with a 3N HCl solution until pH is neutral. The precipitate was filtered, washed several times with water and dried under reduced pressure to give a beige solid. Yield: 55%. M.p.: 195–197 °C (dec.). ^{1}H NMR (DMSO): δ 8.54 (s, 1H, =CH); 8.08 (s, 1H, Ar–H); 7.76 (d, 1H, Ar–H); 7.64 (d, 1H, Ar–H); 7.28–7.21 (m, 5H, Ar–H); 5.00 (t, br, 1H, OH); 4.40 (t, 2H, CH_2); 4.21 (s, 2H, CH_2); 4.10 (s, 2H, CH_2); 3.72 (q, 2H, CH_2); 1.27 (t, 3H, CH_3). Anal. Calcd. for $C_{21}H_{21}NO_4$: C 71.78, H 6.02, N 3.99. Found: C 71.60, H 6.41, N 4.02. ESI/MS (+, m/z): 352.4 [MH^+].

6-Benzyl-1-(2-hydroxyethyl)-4-oxo-1,4-dihydroquinoline-3-carboxylic acid, **HL^1**

A solution of **(2)** (3.35 g, 10.9 mmol) and 2% NaOH (11 mL) was refluxed for 3H and then acidified at r.t. by using 1N HCl. The precipitate was filtered off and recrystallized from water/ethanol giving rise to a white powder. Yield: 97%. M.p.: 187–188 °C (dec.). IR (cm^{-1}): ν_{OH} = 3312; $\nu_{C=O}$ = 1697, 1610. ^{1}H NMR (DMSO): δ 15.32 (s, br, 1H, OH); 8.86 (s, 1H, =CH); 8.23 (s, 1H, Ar–H); 8.02 (d, 1H, Ar–H); 7.83 (d, 1H, Ar–H); 7.30–7.21 (m, 5H, Ar–H); 5.02 (t, br, 1H, OH); 4.60 (t, 2H, CH_2); 4.17 (s, 2H, CH_2); 3.74 (q, 2H, CH_2). ^{13}C NMR (DMSO-d_6): δ 178.2, 166.6, 144.8, 140.6, 139.9, 138.1, 135.1, 128.9, 128.7, 126.3, 124.5, 124.1, 120.0, 107.5, 40.6. Anal. Calcd. for $C_{19}H_{17}NO_4$: C 70.58, H 5.30, N 4.33. Found: C 70.39, H 5.27, N 4.20. ESI/MS (+, m/z): 324.3 [MH^+]. Crystallization from chloroform afforded crystals suitable for X-ray diffraction analysis.

[RuCl(η^6-p-cym)L^1], **(3)**

HL^1 (100 mg, 0.3 mmol) was suspended in 15 ml of methanol, and 12 mg (0.3 mmol) of NaOH (s) was added. The clear solution was stirred 30 min at r.t. and then 92 mg (0.15 mmol) of [Ru(*p*-cym)Cl_2]$_2$ (s) was added. The orange solution was stirred at r.t. overnight, then the solvent was eliminated. The residue was dissolved in dichloromethane and filtered on celite. The filtrate was collected and the solvent was removed under vacuum. The crude product was triturated with *n*-pentane to afford a yellow powder. Yield: 54%. IR (cm^{-1}): ν_{OH} = 3733; $\nu_{C=O}$ = 1614, 1587, 1479. ^{1}H NMR (CD_2Cl_2): δ 8.82 (s, 1H, =CH), 8.31 (s, 1H, Ar–H), 7.62 (s, 2H, Ar–H), 7.33–7.26 (m, 5H, Ar–H), 5.56 (d, 2H, *p*-cym), 5.27 (d, br, 2H, *p*-cym), 4.90 (s, br, OH), 4.37 (s, 2H, CH_2), 4.17 (s, 2H, CH_2), 3.84 (s, 2H, CH_2), 2.92 (m, 1H, CH *p*-cym), 2.10 (s, 3H, CH_3 *p*-cym), 1.33–1.24 (d, 6H, $(CH_3)_2$CH *p*-cym). Anal. Calcd. for $C_{29}H_{30}ClNO_4Ru \cdot H_2O$: C 57.00, H 5.28, N 2.29. Found: C 57.35, H 5.60, N 2.00. ESI/MS (+, m/z): 558.2 [M–Cl]$^+$. Crystals suitable for X-ray diffraction analysis were obtained by slow evaporation of a solution of **(3)** in dichloromethane/*n*-pentane.

[RuCl(η^6-p-cym)L^2], **(4)**

HL^2 was deprotonated before reacting with Ru(II): the ligand was suspended in water and 1.3 equivalents of NaOH (s) were added. The clear solution was stirred at r.t. for 30 min, then the solvent was eliminated under vacuum. The crude solid was dissolved in

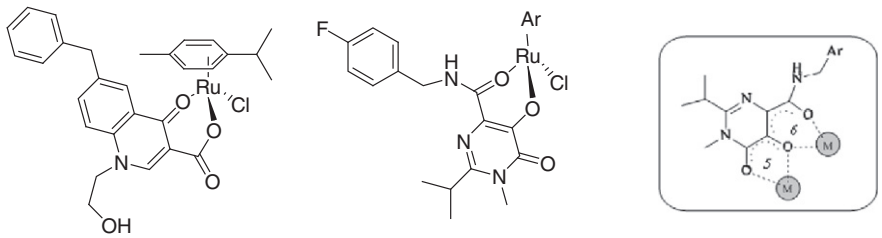

Scheme 2. The Ru(II)–arene complexes.

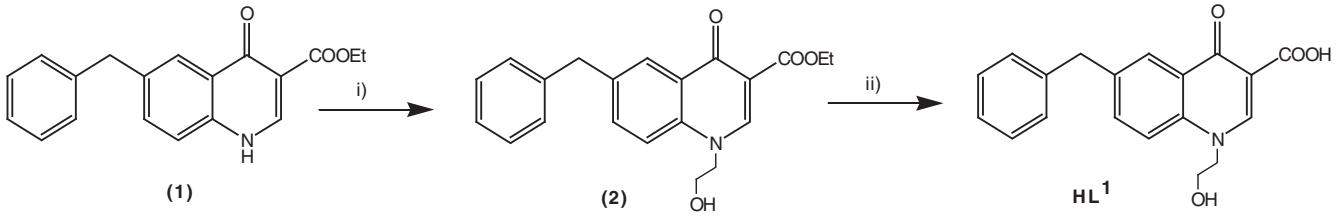

Scheme 3. Preparation of the ligand HL^1. Reagents and conditions: i) NaH 60%, ICH_2CH_2OH, dry DMF, 90 °C for 24 hours; ii) NaOH 2%, refluxing 3 h, then HCl 1N.

dichloromethane, filtered, and the solvent was then eliminated. The residue was triturated with diethyl ether. The sodium salt of the ligand (80 mg, 0.23 mmol) was dissolved in 10 mL of methanol and solid $[RuCl_2(\eta^6\text{-}p\text{-cym})]_2$ (72 mg, 0.11 mmol) was added. The yellow solution was stirred at r.t. overnight, the solvent was eliminated, the residue was dissolved in dichloromethane and filtered on celite. The filtrate was collected, the solvent was removed under vacuum and then the crude product was triturated with diethyl ether to afford an orange powder. Yield: 72%. IR (cm^{-1}): $\nu_{NH} = 3338$; $\nu_{C=O} = 1666$, 1595. ^1H NMR ($CDCl_3$): major isomer, δ 9.54 (s, br, 1H, NH), 7.40–7.30 (m, overlapping signals, Ar–H), 7.09–7.02 (m, overlapping signals, Ar-H), 5.52 (m, overlapping signals, CH *p*-cym), 5.24 (m, overlapping signals, CH *p*-cym), 4.90 (dd, diastereotopic CH_2), 4.38 (dd, diastereotopic CH_2), 3.66 (s, 3H, CH_3), 3.0–2.86 (m, overlapping signals, CH), 2.78–2.74 (m, 1H, CH), 2.18 (s, 3H, CH_3 *p*-cym), 1.34–1.29 (dd, 12H, (CH_3)CH ligand and $(CH_3)_2$CH *p*-cym). Minor isomer, δ 8.29 (s, br, NH), 4.62 (d, CH_2), 3.45 (s, CH_3), 2.27 (s, CH_3 *p*-cym), 1.17–1.15 (m, $(CH_3)_2$CH p-cym). $^{19}F\{^1H\}$-NMR ($CDCl_3$): δ major isomer, −115.88; minor isomer, −114.97. Anal. Calcd. for $C_{26}H_{31}ClFN_3O_3Ru\cdot 0.5H_2O$: C 52.21, H 5.39, N 7.02. Found: C 52.15, H 5.34, N 6.76. ESI/MS (+, m/z): 589.9 $[MH]^+$; 553.1 $[M-Cl]^+$; 454.8 [M-p-cym]$^+$. Crystals suitable for X-ray diffraction analysis were obtained by slow evaporation of a solution of **(4)** in dichloromethane/*n*-hexane.

[RuCl(hexamethylbenzene)L²], **(5)**

The same as **(4)**, by using $[RuCl_2(\text{hexamethylbenzene})]_2$. Orange powder. Yield: 75%. IR (cm^{-1}): $\nu_{NH} = 3225$; $\nu_{C=O} = 1652$, 1598. ^1H NMR (CD_2Cl_2): major isomer, δ 9.73 (s, br, 1H, NH), 7.44–7.36 (m, overlapping signals, Ar–H), 7.10 (m, br, overlapping signals, Ar–H), 4.91 (dd, 2H, diastereotopic CH_2), 4.35 (dd, 2H, diastereotopic CH_2), 3.65 (s, 3H, CH_3), 3.0 (m, br, 1H, CH), 2.0 (s, overlapping signals, CH_3 hexamethylbenz.), 1.36–1.27 (dd, 6H, $(CH_3)_2$CH). Minor isomer, δ 8.32 (s, br, NH), 4.66 (d, CH_2), 3.45 (s, CH_3), 2.92 (m, br, 1H, $(CH_3)_2CH$), 1.19 (dd, $(CH_3)_2$CH). $^{13}C\{^1H\}$-NMR (CD_2Cl_2): major isomer, 169.6; 164.4; 163.3; 160.9; 154.8; 147.4; 135.20; 130.2, 130.1; 115.4; 115.2;88.7; 42.7; 31.0; 31.0 (overlapping signals); 20.9 (overlapping signals); 15.5; minor isomer: 168.0; 162.1; 153.7; 147.1; 133.7; 128.7; 128.6; 115.6; 115.5; 90.3; 43.0; 14.1. $^{19}F\{^1H\}$-NMR (CD_2Cl_2): δ major isomer, −116.56; minor isomer, −116.23. Anal. Calcd. for $C_{30}H_{39}ClFN_3O_3Ru\cdot 0.5H_2O$: C 53.71, H 5.80, N 6.71. Found: C 53.70, H 5.89, N 6.57.

2.3. X-ray crystallography

Single crystal X-ray diffraction data were collected at T = 293 K using the MoKα radiation (λ = 0.71073 Å) on a SMART APEX2 diffractometer for **(3)** and **(4)**, and on a Siemens AED diffractometer equipped with scintillation detector and CuKα radiation (λ = 1.54178 Å) for HL^1. Lorentz, polarization, and absorption corrections were applied [47,48]. Structures were solved by direct methods using SIR97 [49] and refined by full-matrix least-squares on all F^2 using SHELXL97 [50] implemented in the WinGX package [51]. Hydrogen atoms were introduced in calculated positions for **(3)** and **(4)**, and were found on difference maps and refined for HL^1. Anisotropic displacement parameters were refined for all non-hydrogen atoms. Molecule **(4)** is chiral on the ruthenium atom and undergoes spontaneous resolution by crystallizing in the acentric $P2_1$ monoclinic space group. However the crystals were all affected by severe racemic twinning, that was refined by the TWIN/BASF instructions in Shelxl; the twinned component refined to 0.65/0.35 and residuals reproducing the centrosymmetric ghost image were found in the final Fourier difference map. Hydrogen bonds have been analyzed with SHELXL97 [50] and PARST97 [51] and extensive use was made of the Cambridge Crystallographic Data Centre packages [52,53] for the

Table 1
Crystal data and structure refinement for HL^1, **(3)** and **(4)**.

	HL^1	**(4)**	**(3)**
Empirical formula	$C_{19}H_{17}NO_4$	$C_{26}H_{31}ClFN_3O_3Ru$	$C_{29}H_{30}ClNO_4Ru$
Formula weight	323.34	589.06	593.06
Crystal system	monoclinic	monoclinic	triclinic
Space group	$P2_1/c$	$P2_1$	P-1
a/Å	22.861(2)	10.3817(7)	12.662(2)
b/Å	4.9769(1)	10.1538(7)	13.369(2)
c/Å	14.0769(8)	12.7994(9)	18.519(3)
α/°			69.875(3)
β/°	87.102(2)	100.009(1)	81.063(3)
γ/°			61.999(3)
Volume/Å^3	1599.6(2)	1328.7(2)	2598.9(8)
Z	4	2	4
ρ_{calc} mg/mm^3	1.343	1.472	1.516
μ/mm^{-1}	0.777	0.729	0.742
F(000)	680.0	604.0	1216.0
2θ range for data collection	7.74–139.78°	3.24–52.74°	3.64–48.5°
Reflections collected	2935	15965	19584
Independent reflections	2869 [R(int) = 0.0314]	5413 [R(int) = 0.0314]	8335 [R(int) = 0.0481]
Data/restraints/parameters	2869/0/285	5413/17/293	8335/0/651
Goodness-of-fit on F^2	0.941	1.060	1.037
Final R1, wR2 [I >= 2σ (I)]	0.0451, 0.1054	0.0679, 0.1938	0.0570, 0.1487
Final R1, wR2 [all data]	0.0746, 0.1221	0.0789, 0.2137	0.0856, 0.1680
Largest ΔF max/min e Å^{-3}	0.13/−0.18	2.21/−0.51	1.40/−0.69

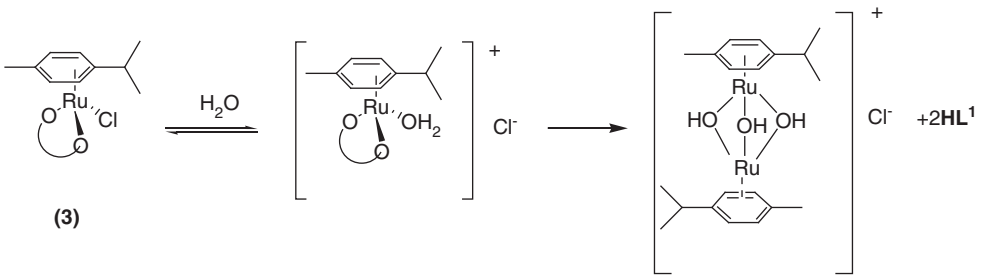

Scheme 4. Hydrolysis of complex **(3)**.

analysis of crystal packing. Table 1 summarizes crystal data and structure determination results. Crystallographic data (excluding structure factors) for HL^1, **(4)** and **(3)** have been deposited with the Cambridge Crystallographic Data Centre as supplementary publication CCDC 878234–878236. Copies of the data can be obtained free of charge on application to CCDC, 12 Union Road, Cambridge CB2 1EZ, UK (fax: (+44) 1223-336-033; e-mail: deposit@ccdc.cam.ac.uk).

2.4. Biological materials, chemicals, and enzymes

All compounds were dissolved in DMSO and the stock solutions were stored at −20 °C. The γ[^{32}P]-ATP was purchased from PerkinElmer. The expression system for wild-type IN was a generous gift of Dr. Robert Craigie, Laboratory of Molecular Biology, NIDDK, NIH, Bethesda, MD.

2.5. Preparation of oligonucleotide substrates

The oligonucleotides 21top, 5′-GTGTGGAAAATCTCTAGCAGT-3′ and 21bot, 5′-ACTGCTAGAGATTTTCCACAC-3′ were purchased from Norris Cancer Center Core Facility (University of Southern California) and purified by UV shadowing on polyacrylamide gel. To analyze the extent of 3′-P and ST using 5′-end labeled substrates, 21top was 5′-end labeled using T_4 polynucleotide kinase (Epicentre, Madison, WI) and γ [^{32}P]-ATP (Amersham Biosciences or ICN). The kinase was heat-inactivated and 21bot was added in 1.5-molar excess. The mixture was heated at 95 °C, allowed to cool slowly to room temperature, and run through a spin 25 mini-column (USA Scientific) to separate annealed double-stranded oligonucleotide from unincorporated material.

2.6. Integrase assays

To determine the extent of 3′-P and ST, wild-type IN was preincubated at a final concentration of 200 nM with the inhibitor in reaction buffer (50 mM NaCl, 1 mM HEPES, pH 7.5, 50 μM EDTA, 50 μM dithiothreitol, 10% glycerol (w/v), 7.5 mM $MnCl_2$, 0.1 mg/ml bovine serum albumin, 10 mM 2-mercaptoethanol, 10% DMSO, and 25 mM MOPS, pH 7.2) at 30 °C for 30 min (HEPES, 4-(2-hydroxyethyl)-1-piperazine ethanesulfonic acid; MOPS, 3-(N-morpholino)propanesulfonic acid). Then, 20 nM of the 5′-end ^{32}P-labeled linear oligonucleotide substrate was added, and incubation was continued for an additional 1 h. Reactions were quenched by the addition of an equal volume (16 μL) of loading dye (98% deionized formamide, 10 mM EDTA, 0.025% xylene cyanol and 0.025% bromophenol blue). An aliquot (5 μL) was electrophoresed on a denaturing 20% polyacrylamide gel (0.09 M tris-borate pH 8.3, 2 mM EDTA, 20% acrylamide, 8 M urea).

Gels were dried, exposed in a PhosphorImager cassette, analyzed using a Typhoon 8610 Variable Mode Imager (Amersham Biosciences) and quantitated using ImageQuant 5.2. Percent inhibition (% I) was calculated using the following equation:

$$\% I = 100\, X\, [1-(D-C)/(N-C)]$$

where *C*, *N*, and *D* are the fractions of 21-mer substrate converted to 19-mer (3′-proc product) or ST products for DNA alone, DNA plus IN, and DNA plus IN plus drug, respectively. The IC_{50} values were determined by plotting the logarithm of drug concentration *versus* percent inhibition to obtain concentration that produced 50% inhibition.

2.7. Cell culture

The MCF7 breast cancer cell line was purchased from the American Type Cell Culture. Cells were maintained in culture under 35 passages and tested regularly for *mycoplasma* contamination using Plasmo TestTM (InvivoGen). Cells were maintained as monolayer cultures in Dulbecco's Modified Eagle Medium (DMEM) containing 10% heat-inactivated fetal bovine serum and supplemented with 2 mmol/L L-glutamine at 37 °C in a humidified atmosphere of 5% CO_2. For subculture and experiments cells were washed with 1× DPBS, detached using 0.025% Trypsin-EDTA (Cellgro), collected in growth media and centrifuged. All experiments were performed in growth media using subconfluent cells in the exponential growth phase.

2.8. Cytotoxicity assays

Cytotoxicity was assessed by a 3-(4,5-dimethylthiazol-2-yl)-2,5-diphenyltetrazolium bromide (MTT) assay as previously described [54]. Briefly, cells were seeded in 96-well microtiter plates and allowed to adhere overnight. Cells were subsequently treated with continuous exposure to the corresponding drug for 72 h. A MTT solution (at a final concentration of 0.5 mg/mL) was added to each well, and cells were incubated for 4 h at 37 °C. After removal of the

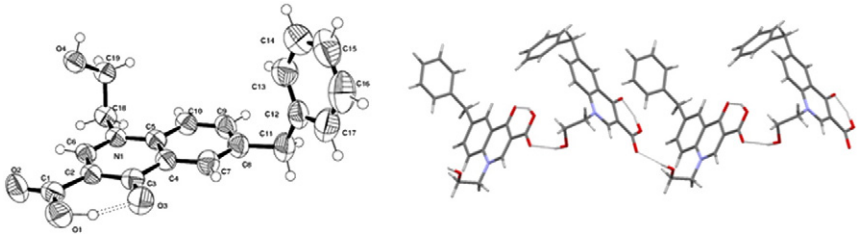

Fig. 1. Molecular structure and labeling of HL^1, with thermal displacement ellipsoids drawn at the 50% probability level (left), and crystal packing with hydrogen bonds displayed as dashed lines (right).

medium, DMSO was added and the absorbance was read at 570 nm. All assays were done in triplicate. The CC_{50} was then determined for each drug from a plot of log (drug concentration) *versus* percentage of cells killed.

3. Results and discussion

3.1. Chemistry

HL^1 was prepared according to Scheme 3, while HL^2 was synthesized as previously reported [13]. The ruthenium(II) complexes **(3)**, **(4)** and **(5)** (Scheme 2) were obtained by reacting in methanol at room temperature $[RuCl_2(\eta^6\text{-}p\text{-cym})]_2$ or $[RuCl_2(\eta^6\text{-hexamethylbenzene})]_2$ with two equivalents of the ligand, that was previously deprotonated with NaOH. The Ru(II) complexes have been isolated as yellow–orange powders in high yields and they show good solubility in chlorinated and alcoholic solvents. Their full characterization has been obtained by spectroscopic methods (NMR, IR), MS, elemental analysis and by single crystal X-ray diffraction analysis.

The data clearly indicate that the ligands are anionic and bidentate, giving rise to pseudo-octahedral organometallic compounds (Scheme 2). In particular, HL^2 has two different compartments that can be involved in coordination, giving rise to five- or six-membered chelation rings (Scheme 2, inset). In the IR spectra of **(4)** and **(5)**, the carbonylic stretching absorption of the secondary amide shifts to lower wave numbers (from 1636 cm^{-1} in HL^2 to 1595 and 1598 cm^{-1} in **(4)** and **(5)**, respectively), as observed in other complexes that we have previously synthesized [13]. This is in accord with the involvement of the secondary amide group in the coordination to the metal ion. Effectively, the X-ray diffraction analysis of **(4)** (*vide infra*) confirms that the deprotonated ligand is coordinated to Ru(II) through the hydroxyl oxygen and the carbonyl oxygen of the secondary amide, while the tertiary amide is excluded by the coordination sphere. The pseudo-octahedral coordination of the metal is then completed by a chloride ion and by the *p*-cymene moiety.

The ^{1}H-NMR spectrum of **(4)** is rather interesting. Apart from the absence of the OH proton and the variation of the chemical shift due to the complexation, in **(4)** Ru is a chiral center, so that the benzylic CH_2 protons are diasterotopic and produce an AB quartet. Moreover, there are two sets of signals, probably due to two different isomers. The presence of two species is confirmed by ^{19}F-NMR in $CDCl_3$, where two signals are detected (at −115.88 and −114.97 ppm for the major and minor isomers, respectively; −114.42 ppm in the free ligand). Crystals of **(4)** were dissolved in CD_2Cl_2 and ^{1}H and ^{19}F $\{^1H\}$-NMR spectra were immediately recorded: they are identical to that obtained by dissolution of the powder. Finally, the spectra were recorded at different temperatures and the *ratio* between the two isomers changes from 1:3 at −30 °C to 1:2 at +50 °C.

In order to simplify the arene on the Ru(II) ion, the hexamethylbenzene analog **(5)** has been synthesized. The ^{1}H- and ^{19}F $\{^1H\}$-NMR spectra of **(5)** are analogous to the ones of **(4)**, showing the presence of two species (see Experimental section). In particular, in the $^{13}C\{^1H\}$-NMR spectrum of **(5)** there are two sets of signals, but no shift of the tertiary amide carbon is observed in comparison with the free ligand. The same situation was found in the $^{13}C\{^1H\}$-NMR spectrum of an X-ray characterized Mg(II) complex, where HL^2 is deprotonated and forms a six-membered chelation ring [13]. This excludes that one of the two species present in the solution of **(5)** can originate by the involvement of the tertiary amide moiety in the coordination to the metal center, with the formation of a five-membered chelation ring (Scheme 2, inset).

It seems reasonable to conclude that the two sets of signals in the spectra of **(4)** and **(5)** are due to the fact that the rotation of the *p*-fluorobenzyl amide chain is hindered by the arene bound to the ruthenium ion.

In the ^{1}H-NMR spectrum of **(3)** only one set of signals is present and the acidic proton is absent. In the IR spectra, the absorption of the ν(C═O) at 1697 cm^{-1} of the free quinolone HL^1 was replaced by two strong bands at 1614 and 1479 cm^{-1}, attributable to the asymmetric and symmetric ν(O–C–O) vibrations, respectively. The pyridone stretching vibration is shifted upon coordination from 1610 cm^{-1} to 1587 cm^{-1}. The changes in the IR spectra suggest that the mono-deprotonated ligand HL^1 chelates Ru(II) through the pyridone and one carboxylate oxygen [13]; the coordination sphere is then completed by a chlorine ion and the *p*-cymene moiety, as observed in other ruthenium(II) complexes with quinolone ligands [40,41]. The structure of **(3)** was confirmed by X-ray analysis on single crystal (*vide infra*).

The solution behavior of ruthenium(II) organometallic compounds in the presence of water is very important, since it can be related to their biological activity. Compound **(4)** was dispersed in D_2O, where it is not completely soluble. In its ^{1}H and $^{19}F\{^1H\}$-NMR spectra there are the signals of a third species containing the ligand still complexed with Ru(II). No variations were observed in the spectra up to 4 days. It is reasonably to suppose that the third set of signals arises from the formation of an aqua-complex, where a water molecule replaces the chlorine ion in the coordination sphere of the metal [40,41].

Compound **(3)** was dispersed in D_2O as well. In this case, in its ^{1}H-NMR spectrum it is possible to observe the presence of signals that can be attributed to a hydroxo-bridged Ru(II) dimer, that is the product of the hydrolysis of the complex, as for analogous half-sandwich ruthenium complexes (Scheme 4) [40,41]. In fact, in addition to the signals of **(3)**, in the *p*-cymene region there are two doublets at 5.27 and 5.05 ppm, a multiplet at 2.56 ppm and a doublet at 1.11 ppm. The hydroxo-complex forms immediately, with a *ratio* of about 0.75:1 between **(3)** and the new species (about 0.55:1 after 24 h).

3.2. X-ray crystallographic studies

The molecular and crystal structures of the free ligand HL^1 are shown in Fig. 1. The benzyl and the hydroxyethyl groups confer a

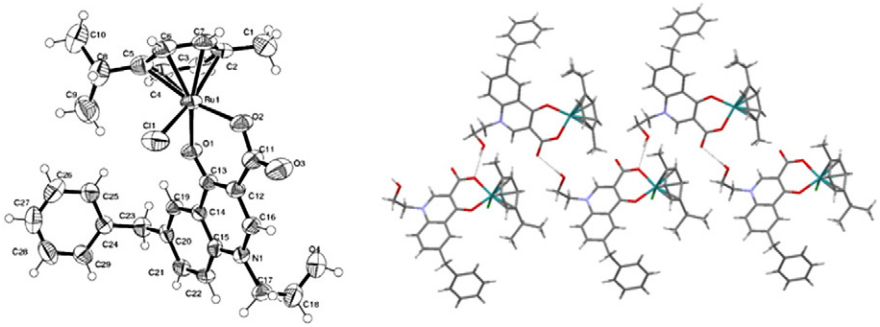

Fig. 2. Molecular structure and labeling of one molecule of **(3)**, with thermal displacement ellipsoids drawn at the 50% probability level (left), and crystal packing with hydrogen bonds displayed as dashed lines (right).

skewed shape to the molecule, whose core is constituted by the planar quinolone system; in fact both are almost perpendicular to the molecular core (C9–C8–C11–C12 = 101°; C6–N1–C18–C19 = 99°), and point out of the same face of the fused rings. The bond geometry is not significantly different from the average values for similar systems [55]. The carboxylic acid OH group is involved in a hydrogen bond, forming an intramolecular six-membered ring (O1–H…O3 = 2.503 (2)Å, 153(3)°) that locks the –COOH potentially rotatable group in the plane of quinolone. The remaining hydrogen bond hydroxyl donor and carboxylic acceptor of HL^1, are employed in an intermolecular hydrogen bond that arranges the crystal packing in arrays along the c axis (Fig. 1, O4–H…O2(x, 1/2 − y, 1/2 + z) = 2.709(2)Å, 164(3)°).

The molecular structure of the corresponding ruthenium complex **(3)** is shown in Fig. 2. The ligands are arranged around ruthenium in a distorted octahedron, with the *p*-cymene ring occupying three positions of the polyhedron of coordination. Two other positions are occupied by the chelating system of HL^1, comprising the deprotonated oxygen of the carboxylic acid and the 4-oxo group. The remaining position is occupied by one chloride ligand. Complex **(3)** crystallizes with two independent molecules in the asymmetric unit, that slightly differ only for the orientation of the *p*-cymene around the bond axis between ruthenium and the center of the *p*-cymene ring (Cl–Ru–C–CH_3 = 71 and 102° in the two cases). The co-crystallization of crystallographic independent conformers differing only in the orientation of the *p*-cymene ring for ruthenium half-sandwich complexes is related to the known fluxionality of the ruthenium–arene bond in solution, and it has already been observed in similar cases [56,57]. Similar to the intramolecular hydrogen bond in the free ligand, here the chelation on ruthenium locks the carboxylate group in the plane of the quinolone system, maintaining the planarity of the molecular core. However, the chelation of ruthenium produces a slight angular deformation of the system, since the C12–C13–O1 bond angle in **(3)** widens (126.9(6) and 125.4(6)° for the two molecules) with respect to the corresponding C2–C3–O3 in HL^1 (122.3(2)°). The six-membered chelation ring adopts an envelope conformation in both independent molecules, forcing the two donor oxygens slightly out of the molecular plane. The ruthenium atoms are 0.64 and 0.50 Å out of the chelation planes in the two cases. Regarding the general molecular shape, the benzylic and hydroxyethyl substituents are nearly perpendicular to the quinoline ring, but with respect to the free ligand the hydroxyethyl group is rotated on the opposite side (C21–C20–C23–C24 = 106 and 101°; C16–N1–C17–C18 = −96 and −93° respectively for the two independent molecules). The hydroxyl groups of the two independent molecules form hydrogen bonds to the coordinated oxygen of the carboxylate groups originating arrays along which the two independent molecules alternate in the crystal packing (Fig. 2).

Complex **(4)** crystallizes in the acentric $P2_1$ space group, due to a spontaneous resolution of the chiral centers on the ruthenium atom. The molecular structure is reported in Fig. 3. The coordination around ruthenium is the same distorted octahedron observed for **(3)**, whereby in **(4)** the chelation is attained by means of the amidic and of the 4-oxo oxygen donors. Due to twinning problems discussed in the Experimental section, the bond geometry is not accurate enough to be compared with related compounds; however it can be noted that the angle C14–C19–O1 = 132.2(8)° is broadened by the chelation, similarly to complex **(3)**. The more flexible nature of the HL^2 ligand with respect to HL^1 results in a general higher deviation from planarity of the complex. The ligand skeleton is much less planar than the one observed for the quinolone ligand in **(3)**, with deviations up to 0.51 Å (O3) and rms deviation of 0.20 Å compared to a rms deviation of 0.06 Å and 0.12 Å with maximum displacements of 0.13 Å (O2) and 0.24 Å (O5) for the two molecules of **(5)**. The six-membered chelation ring has a slightly twisted envelope conformation with ruthenium out of the chelation plane by 0.77 Å. Similarly to HL^1 and to **(3)**, the *p*-fluoro benzylic substituent is almost perpendicular to the average molecular plane (C19–N1–C20–C21 = −96°). The direct

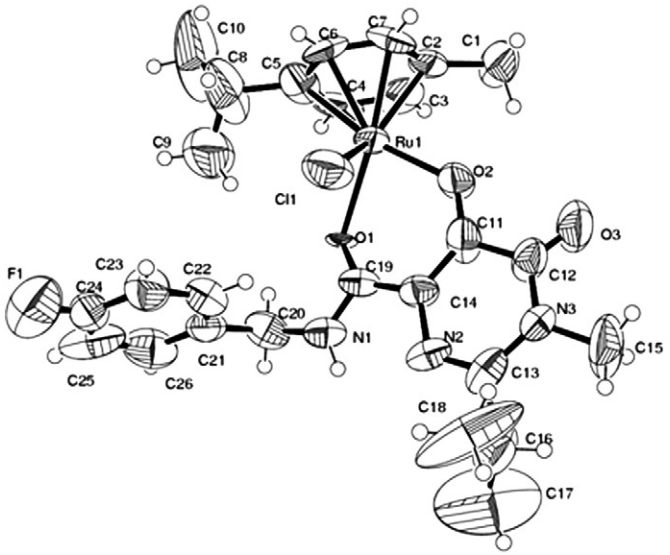

Fig. 3. Molecular structure and labeling of **(4)**, with thermal displacement ellipsoids drawn at the 50% probability level.

comparison of **(3)** and **(4)** shows how the different chelation sites affect the overall molecular shape (Fig. 4). The most significant supramolecular features in the crystal packing of **(4)** are the NH…Cl hydrogen bonds between the amidic NH group and the ruthenium-bound chloride (N1–H…Cl1(1 − x, 1/2 + y, 1 − z) = 3.439(8) Å, 129°). It is well recognized that metal bound halides are very good hydrogen bond acceptors [58] and similar examples of hydrogen bonds to chlorides in half-sandwich ruthenium units have been reported recently [59].

3.3. Inhibition of HIV-1 IN

The ligand HL^1 and the complexes **(3)** and **(4)** were tested for their ability to inhibit 3′-P and ST catalytic activities by employing purified enzyme (Fig. 5). All the compounds showed inhibition potency in sub to low micromolar concentration range (Table 2); $[RuCl_2(p\text{-cym})]_2$ was evaluated for comparison, and it was found inactive up to 500 μM. The ligand HL^2 (IC_{50}, ST = 0.14 ± 0.03 μM; 3′-P = 10 ± 8 μM)

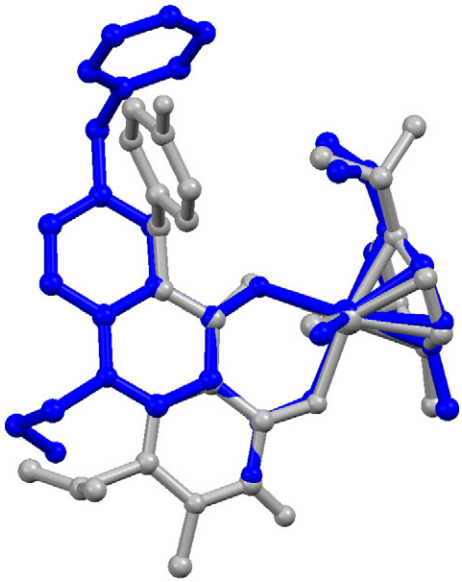

Fig. 4. Comparison of the molecular structures of **(3)** (blue) and **(4)** (gray). Hydrogen atoms are omitted for clarity.

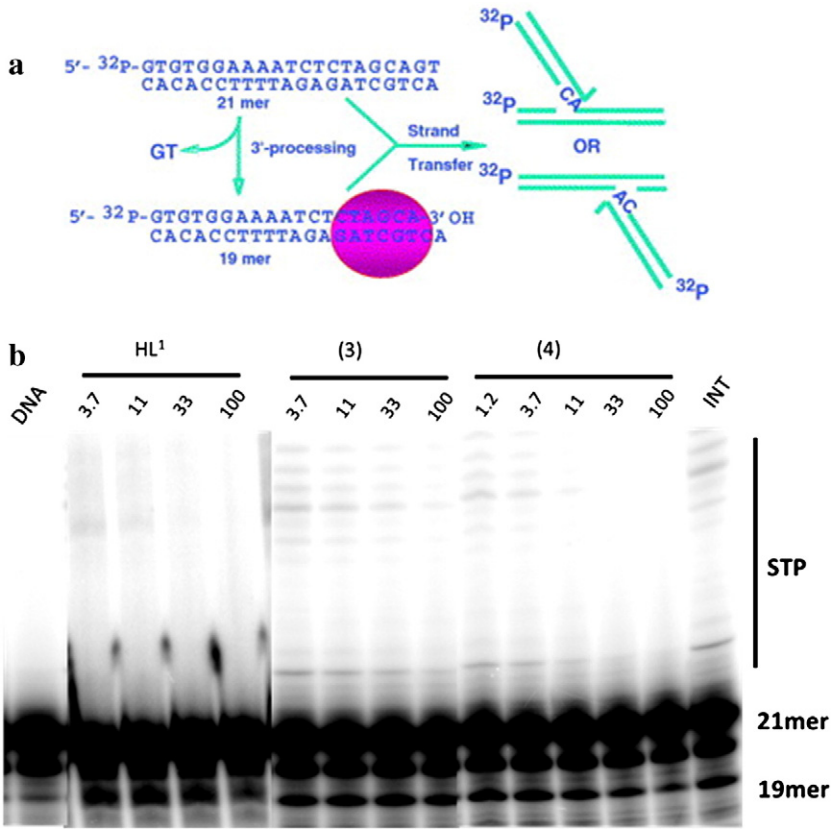

Fig. 5. Schematic representation of IN activity *in vitro* and representative gels showing inhibition of purified IN by HL^1, **(3)** and **(4)**. a) A 21-mer blunt-end oligonucleotide corresponding to the U5 end of the HIV-1 LTR, 5′ end-labeled with ^{32}P, is reacted with purified IN. The first step (3′-P) involves nucleolytic cleavage of two bases from the 3′-end, resulting in a 19-mer oligonucleotide. Subsequently, 3′ ends are covalently joined at several sites to another identical oligonucleotide that serves as the target DNA (ST). The products formed by this reaction migrate slower than the original substrate on a polyacrylamide gel. b) Line named as DNA indicates DNA alone; line termed INT indicates IN and DNA with no drug; other lines: IN, DNA and selected drug concentrations (μM) as indicated in each line.

[13] is about 20 fold more potent than the quinolone HL^1 (IC_{50}, ST = 3.1 ± 1.1 μM; 3′-P = 93 ± 9 μM), confirming a trend that was already observed for similar compounds [13]. **(4)** (IC_{50}, ST = 1.8 ± 0.78 μM; 3′-P = 44 ± 16 μM) resulted the most active complex, even if in the ST process it is about 13 fold less active than the corresponding free ligand HL^2. **(4)** retained selectivity towards ST, with a selectivity index of about 25 (71 for HL^2, Table 2). Also for **(3)**, there is a lowering of the activity in the ST process inhibition of about 5–6 fold with respect to the corresponding free ligand. While **(3)** and **(4)** are less active than the corresponding free ligands, the bis-chelate complexes $[ML^2_2]\cdot nH_2O$ (M = Mg(II), Mn(II), Co(II) and Zn(II)) and $[ML_2]\cdot nH_2O$ (M = Mg(II) and Mn(II); HL: 6-benyl-4-oxo-1,4-dihydroquinolin-3-carboxylic acid, a quinolone similar to HL^1) showed an analogous or even a better inhibition profile [13].

Previously, it was shown that ruthenium(II) arene complexes can show significant cytotoxicity in several cancer cell lines [2–6]. Therefore, HL^1, HL^2, **(3)** and **(4)** were also tested for their cytotoxicity against a model breast cancer cell line (MCF7, Table 2): none of them showed antiproliferative activity (CC_{50} > 20 μM) at concentration values higher than their enzymatic inhibition activity values.

It is worth noting that **(3)** and **(4)** are, as far as we know, the first ruthenium complexes with a significant activity against HIV-1 IN.

Table 2
Inhibition of HIV-1 IN activity and cytotoxicity of ligands and complexes.

Compound	HIV-1 integrase inhibition IC_{50} (μM)		[a]SI	[b]MCF7 [c]CC_{50} (μM)
	3′-Processing	Strand transfer		
HL^1	93 ± 9	3.1 ± 1.1	30	> 20
HL^2	10 ± 8	0.14 ± 0.03	71.4	> 20
(3)	> 100	17 ± 7	> 5.9	> 20
(4)	44 ± 16	1.8 ± 0.78	24.4	> 20

[a] SI, Selectivity Index.
[b] MCF7, breast cancer cell line.
[c] CC_{50}, cytotoxic concentration 50%.

4. Conclusions

The new ruthenium complexes **(3)**, **(4)** and **(5)** were synthesized, characterized and the X-ray diffraction structures of **(3)** and **(4)** were discussed. **(3)** was one of the few examples of ruthenium quinolone complexes, a class of compounds recently studied also for their anticancer properties [41]. Although **(3)** and **(4)** demonstrated good inhibition against HIV IN, the Ru(II) arene moiety did not contribute to enhance significantly the intrinsic activity of the parent ligands HL^1 and HL^2. However **(3)** and **(4)** resulted among the few Ru(II) complexes active against HIV [7–9] and, in particular, the first ones that were active against HIV IN. The activity of **(3)** was influenced by the partial hydrolysis of the complex in aqueous solution (see NMR experiments) with release of HL^1. On the other hand, the activity of **(4)**, that was quite stable in aqueous solution, seemed to be due to the complex, that evidently was able to influence HIV IN activity.

The metal complexes can inhibit the activity of HIV-1 IN by carrying the ligand inside the active site of the enzyme, where the ligand can interfere with the magnesium metal cofactors. Nevertheless, on the basis of the available data, assertions about the mechanism of inhibition of HIV IN by the metal complexes are inevitably speculative.

Acknowledgments

The authors thank the "Centro Interfacoltà Misure *Giuseppe Casnati*" and the "Laboratorio di Strutturistica *Mario Nardelli*" of the University of Parma for facilities. This study was supported in part by funds from the grant CRP-25920, within the frame of "Legge regionale n. 7/2007, promozione della ricerca scientifica e dell'innovazione tecnologica in Sardegna — Annualità 2010"; Regione Autonoma della Sardegna is gratefully acknowledged.

Appendix A. Supplementary data

Supplementary data to this article can be found online at http://dx.doi.org/10.1016/j.jinorgbio.2012.09.021.

References

[1] C. Orvig, M.J. Abrams, Chem. Rev. 99 (1999) 2201–2203.
[2] C.G. Hartinger, P.J. Dyson, Chem. Soc. Rev. 38 (2009) 391–401.
[3] P.C.A. Bruijnincx, P.J. Sadler, Curr. Opin. Chem. Biol. 12 (2008) 197–206.
[4] R. Wai-Yin Sun, D.-L. Ma, E.L.-M. Wong, C.-M. Che, Dalton Trans. (2007) 4884–4892.
[5] A. Bergamo, G. Sava, Dalton Trans. 40 (2011) 7817–7823.
[6] Y.K. Yan, M. Melchart, A. Habtemariam, P.J. Sadler, Chem. Commun. (2005) 4764–4776.
[7] N.W. Luedtke, J.S. Hwang, E.C. Glazer, D. Gut, M. Kol, Y. Tor, Chem. BioChem. 3 (2002) 766–771.
[8] L. Mishra, R. Sinha, H. Itokawa, K.F. Bastow, Y. Tachibana, Y. Nakanishi, N. Kilgore, K.-H. Lee, Bioorg. Med. Chem. 9 (2001) 1667–1671.
[9] E.L.-M. Wong, R.W.-Y. Sun, N.P.-Y. Chung, C.-L.S. Lin, N. Zhu, C.-M. Che, J. Am. Chem. Soc. 128 (2006) 4938–4939.
[10] M. Sechi, A. Bacchi, M. Carcelli, C. Compari, E. Duce, E. Fisicaro, D. Rogolino, P. Gates, M. Derudas, L.Q. Al-Mawsawi, N. Neamati, J. Med. Chem. 49 (2006) 4248–4260.
[11] A. Bacchi, M. Biemmi, M. Carcelli, F. Carta, C. Compari, E. Fisicaro, D. Rogolino, M. Sechi, M. Sippel, C. Sotriffer, T. Sanchez, N. Neamati, J. Med. Chem. 51 (2008) 7253–7264.
[12] A. Bacchi, M. Carcelli, C. Compari, E. Fisicaro, N. Pala, G. Rispoli, D. Rogolino, T.W. Sanchez, M. Sechi, N. Neamati, Mol. Pharm. 8 (2011) 507–519.
[13] A. Bacchi, M. Carcelli, C. Compari, E. Fisicaro, N. Pala, G. Rispoli, D. Rogolino, T.W. Sanchez, M. Sechi, V. Sinisi, N. Neamati, J. Med. Chem. 54 (2011) 8407–8420.
[14] N. Neamati, HIV-1 Integrase: Mechanism and Inhibitor Design, J. Wiley&Sons, Hoboken, NJ, USA, 2011. ed.
[15] V. Nair, G. Chi, Rev. Med. Virol. 17 (2007) 277–295.
[16] R. Dayam, L.Q. Al-Mawsawi, N. Neamati, Drugs R. D. 8 (2007) 155–168.
[17] L.Q. Al-Mawsawi, R.I. Al-Safi, N. Neamati, Expert Opin. Emerg. Drugs 13 (2008) 213–225.
[18] N. Prada, M. Markowitz, Expert Opin. Investig. Drugs 19 (2010) 1087–1098.
[19] MK-0518 meeting transcript. Department of Health and Human Services; Food and Drug Administration; Center for Drug Evaluation and Research; Antiviral Drugs Advisory Committee; 2007 September 5. Available from www.fda.gov/ohrms/dockets/ac/cder07.htm#AntiviralDrugs.
[20] E.P. Garvey, B.A. Johns, M.J. Gartland, S.A. Foster, W.H. Miller, R.G. Ferris, R.J. Hazen, M.R. Underwood, E.E. Boros, J.B. Thompson, J.G. Weatherhead, C.S. Koble, S.H. Allen, L.T. Schaller, R.G. Sherrill, T. Yoshinaga, M. Kobayashi, C. Wakasa-Morimoto, S. Miki, K. Nakahara, T. Noshi, A. Sato, T. Fujiwara, Antimicrob. Agents Chemother. 52 (2008) 901–908.
[21] E.E. Boros, C.E. Edwards, S.A. Foster, M. Fuji, T. Fujiwara, E.P. Garvey, P.L. Golden, R.J. Hazen, J.L. Jeffrey, B.A. Johns, T. Kawasuji, R. Kiyama, C.S. Koble, N. Kurose, W.H. Miller, A.L. Mote, H. Murai, A. Sato, J.B. Thompson, M.C. Woodward, T. Yoshinaga, J. Med. Chem. 52 (2009) 2754–2761.
[22] M. Rowley, Prog. Med. Chem. 46 (2008) 1–28.
[23] V. Summa, A. Petrocchi, F. Bonelli, B. Crescenzi, M. Donghi, M. Ferrara, F. Fiore, C. Gardelli, P.O. Gonzalez, D.J. Hazuda, P. Jones, O. Kinzel, R. Laufer, E. Monteagudo, E. Muraglia, E. Nizi, F. Orvieto, P. Pace, G. Pescatore, R. Scarpelli, K. Stillmock, M.V. Witmer, M. Rowley, J. Med. Chem. 51 (2008) 5843–5855.
[24] M. Sato, T. Motomura, H. Aramaki, T. Matsuda, M. Yamashita, Y. Ito, H. Kawakami, Y. Matsuzaki, W. Watanabe, K. Yamataka, S. Ikeda, E. Kodama, M. Matsuoka, H. Shinkai, J. Med. Chem. 49 (2006) 1506–1508.
[25] R. Dayam, L.Q. Al-Mawsawi, Z. Zawahir, M. Witvrouw, Z. Debyser, N. Neamati, J. Med. Chem. 51 (2008) 1136–1144.
[26] M. Kobayashi, T. Yoshinaga, T. Seki, C. Wakasa-Morimoto, K.W. Brown, R. Ferris, S.A. Foster, R.J. Hazen, S. Miki, A. Suyama-Kagitani, S. Kawauchi-Miki, T. Taishi, T. Kawasuji, B.A. Johns, M.R. Underwood, E.P. Garvey, A. Sato, T. Fujiwara, Antimicrob. Agents Chemother. 55 (2011) 813–821.
[27] R. Kiyama, T. Kawasuji, PCT Int. Appl, 2001. WO-01/95905.
[28] B.A. Johns, A.C. Svolto, Expert Opin. Ther. Patents 18 (2008) 1225–1237
[29] L.A. Mitscher, Chem. Rev. 105 (2005) 559–592.
[30] I. Laponogov, M.K. Sohi, D.A. Veselkov, X.S. Pan, R. Sawhney, A.W. Thompson, K.E. McAuley, L.M. Fisher, M.R. Sanderson, Nat. Struct. Biol. 16 (2009) 667–669.
[31] P. Drevenšek, I. Turel, N. Poklar Ulrih, J. Inorg. Biochem. 96 (2003) 407–415.
[32] N. Jimenez-Garrido, L. Perello, R. Ortiz, G. Alzuet, M. Gonzalez-Alvarez, E. Canton, M. Liu-Gonzalez, S. Garcia-Granada, M. Perez-Priede, J. Inorg. Biochem. 99 (2005) 677–689.
[33] M.E. Katsarou, E.K. Efthimiadou, G. Psomas, A. Karaliota, D. Vourloumis, J. Med. Chem. 51 (2008) 470–478.
[34] I. Turel, Coord. Chem. Rev. 232 (2002) 27–47.
[35] S.A. Sadeek, J. Mol. Struct. 753 (2005) 1–12.
[36] P. Drevenšek, J. Košmrlj, G. Giester, T. Skauge, E. Sletten, K. Sepčić, I. Turel, J. Inorg. Biochem. 100 (2006) 1755–1763.
[37] I. Turel, P. Živec, A. Pevec, S. Tempelaar, G. Psomas, Eur. J. Inorg. Chem. (2008) 3718–3727.
[38] S. Lecomte, M.H. Baron, M.T. Chenon, C. Coupry, N.J. Moreau, Antimicrob. Agents Chemother. 38 (1994) 2810–2816.
[39] A. Wohlkonig, P.F. Chan, A.P. Fosberry, P. Homes, J. Huang, M. Kranz, V.R. Leydon, T.J. Miles, N.D. Pearson, R.L. Perera, A.J. Shillings, M.N. Gwynn, B.D. Bax, Nat. Struct. Mol. Biol. 17 (2010) 1152–1153.
[40] I. Turel, J. Kljun, F. Perdih, E. Morozova, V. Bakulev, N. Kasyanenko, J.A.W. Byl, N. Osheroff, Inorg. Chem. Commun. 49 (2010) 10750–10752.
[41] J. Kljun, A.K. Bytzek, W. Kandioller, C. Bartel, M.A. Jakupec, C.G. Hartinger, B.K. Keppler, I. Turel, Organometallics 30 (2011) 2506–2512.
[42] M. Badea, R. Olar, D. Marinescu, V. Uivarosi, D. Jacob, J. Therm. Anal. Calorim. 97 (2009) 735–739.
[43] M. Badea, R. Olar, D. Marinescu, V. Uivarosi, T.O. Nicolescu, D. Jacob, J. Therm. Anal. Calorim. 99 (2010) 829–834.
[44] C.J. Sunderland, M. Botta, S. Aime, K.N. Raymond, Inorg. Chem. 40 (2001) 6746–6756.
[45] C.A. Vock, W.H. Ang, C. Scolaro, A.D. Phillips, L. Lagopoulos, L. Juillerat-Jeanneret, G. Sava, R. Scopelliti, P.J. Dyson, J. Med. Chem. 50 (2007) 2166–2175.
[46] W.H. Ang, A. De Luca, C. Chapuis-Bernasconi, L. Juillerat-Jeanneret, M. Lo Bello, P.J. Dyson, Chem. Med. Chem. 2 (2007) 1799–1806.
[47] SAINT: SAX, Area Detector Integration, Siemens Analytical Instruments Inc., Madison, Wisconsin, USA.
[48] SADABS: Siemens Area Detector Absorption Correction Software, Sheldrick G., 1996, University of Goettingen, Germany.
[49] Sir97: A new program for solving and refining crystal structures — Altomare, A.; Burla, M.C.; Cavalli, M.; Cascarano, G.; Giacovazzo, C.; Gagliardi, A.; Moliterni, A.G.; Polidori, G.; Spagna, R., 1997, Istituto di Ricerca per lo Sviluppo di Metodologie Cristallografiche CNR, Bari.
[50] Shelxl97. Program for structure refinement. Sheldrick G., University of Goettingen, Germany, 1997.
[51] L.J. Farrugia, J. Appl. Crystallogr. 32 (1999) 837–838.
[52] F.H. Allen, O. Kennard, R. Taylor, Acc. Chem. Res. 16 (1983) 146–153.
[53] I.J. Bruno, J.C. Cole, P.R. Edgington, M. Kessler, C.F. Macrae, P. McCabe, J. Pearson, R. Taylor, Acta Crystallogr. B58 (2002) 389–397.
[54] J. Carmichael, W.G. DeGraff, A.F. Gazdar, J.D. Minna, J.B. Mitchell, Cancer Res. 47 (1987) 936–942.
[55] I.J. Bruno, J.C. Cole, M. Kessler, Jie Luo, W.D.S. Motherwell, L.H. Purkis, B.R. Smith, R. Taylor, R.I. Cooper, S.E. Harris, A.G. Orpen, J. Chem. Inf. Comput. Sci. 44 (2004) 2133–2144.
[56] T.A. Albright, Acc. Chem. Res. 15 (1982) 149–155.
[57] A. Bacchi, G. Cantoni, F. Mezzadri, P. Pelagatti, Cryst. Growth Des. 12 (2012) 4240–4247.
[58] L. Brammer, E.A. Bruton, P. Sherwood, Cryst. Growth Des. 4 (2001) 277–290.
[59] A. Bacchi, G. Cantoni, M.R. Chierotti, A. Girlando, R. Gobetto, G. Lapadula, P. Pelagatti, A. Sironi, M. Zecchini, Cryst. Eng. Com. 13 (2011) 4365–4375.